AUT Journal of Civil Engineering

AUT J. Civil Eng., 3(2) (2019) 149-156
DOI: 10.22060/ajce.2018.14833.5500

Intelligent Mathematical Modeling of Discharge Coefficient of Nonlinear Weirs with Triangular Plan

A. H. Haghiabi[1*], A. Parsaie[2], Z. Shamsi[3]

[1] Water Engineering Department, Lorestan University, Khorramabad, Iran
[2] Faculty of Water Sciences Engineering, Shahid Chamran University of Ahvaz, Ahvaz, Iran
[3] Department of Water and Soil Conservation, Ministry of Agriculture Jihad, Kerman, Iran

ABSTRACT: In this study, the discharge coefficient (C_d) of non-linear weirs with a triangular plan was mathematically modeled using a group of method data handling (GMDH), genetic programming (GP) and multivariate adaptive regression splines (MARS) techniques. For this purpose, related datasets including parameters on C_d were collected from literature. These methods were selected since they are classified as smart function fitting (SFF) methods. The main advantages of SFF methods compared to other artificial intelligence methods are defining the most effective parameters on output and assigning more weights to them in mathematical expression process. Results of MARS indicated that this method with fifteen basic functions could achieve good accuracy for modeling and predicting C_d (R^2= 0.98 and RMSE=0.024). Results of GMDH showed that this model includes two hidden layers and that there are five and four neurons at the first and second hidden layers, receptivity. Results of developed GP model declared that this model consists of three genes and has acceptable performance for modeling C_d. Evaluation of proficiency of utilized models with each other indicated that the best accuracy is related to MARS model. Calculating the discrepancy ratio index (DDR) shows that the minimum range of DDR is related to MARS model.

Review History:

Received: 15 August 2018
Revised: 19 November 2018
Accepted: 12 December 2018
Available Online: 12 December 2018

Keywords:
DDR Index
Nonlinear Weir
Flow Measurement
Discharge Capacity

1- Introduction

Modeling hydraulic structures is one of the major parts of hydraulic engineering. Among hydraulic structures, weirs have been widely used in hydraulic engineering projects. Modeling the hydraulic behavior of weirs is more important especially when designers decide to use them as flood evacuation system in the earthen dam projects [1]. Nowadays, due to the effect of climate change on river flow regimes and escalation of critical flood conditions, revising the performance of constructed weirs is necessary [2, 3]. In other words, increasing the discharge capacity of existing weirs is necessary. There are several ideas for improving the discharge capacity of weirs, however, the non-linear weirs are very convenient when it is needed to get out a lot of water in the low values of head flow [4-6]. Labyrinth weirs (W_L) are the most famous form of nonlinear weirs. Several shapes such as triangular, trapezoidal, rectangular and piano key have been suggested for the crest of W_L [7]. The first study on W_L was reported by Taylor [8]. He conducted extensive studies on W_L with triangular, triangular and rectangular crest and he realized that the performance of trapezoidal labyrinth weir is more than others. Up to now, several studies on W_L have been reported. The concept of W_L has also been considered for improving the discharge capacity of side weirs [9-17]. Nowadays, W_L has been used in over 200 hydro-system projects especially dam projects and river deviation systems. In this regard, Ute Dam, Loombah Dam, New London Dam, Brazos Dam, Koontz Lake Dam, and Isabella Dam can be mentioned [3, 18, 19]. Based on reports, at low value of head of flow over the crest, the discharge capacity of W_L is about three to five times more than linear weirs. It is notable that the discharge coefficient (C_d) of W_L is less than the sharp linear weirs; however, their high discharge capacity is related to provide the larger length of their crest. Recently by advances in numerical methods such as computational fluid dynamic (CFD) techniques [20, 21] and soft computing methods in most areas of hydraulic engineering [22-24], Investigators have attempted to apply them for modeling the hydraulics of W_L [25]. Using of CFD technique for modeling labyrinth side weirs and W_L was reported by Aydin [26], Aydin and Emiroglu [27], Robertson [28] and Crookston and Tullis [29]. Using soft computing techniques such Artificial Neural Networks (ANN), Genetic Programming (GP), Support Vector Machine and M5 Model Tree, Group Method of Data Handling (GMDH), Adaptive Neuro-Fuzzy Inference System for predicting the hydraulic characteristics of labyrinth side weirs have been reported by [30-39]. An overview of previous studies shows that so far, mathematical modeling of the C_d of W_L based on intelligent methods such as GP, MARS and GMDH has

Corresponding author, E-mail: haghiabi.a@lu.ac.ir

not been reported. Hence, in this paper, these techniques are used for intelligent mathematical expression for C_d of W_L.

2- Materials and Methods

The C_d of triangular W_L is proportional to the geometric and hydraulic parameters. The main effective parameters are shown in Figure 1. In this figure, P is the weir height, W is the main channel width, w is the width of one cycle, h and H are the depth and head of flow over the crest at upstream, respectively. y_0 and E_0 are the total of depth and head of flow at upstream, respectively.

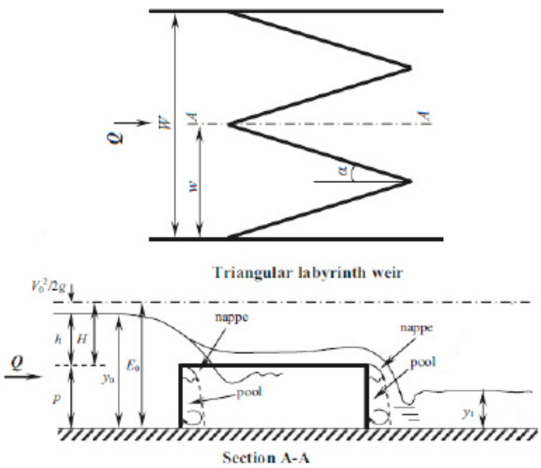

Figure 1. the scheme of labyrinth weir with triangular plans crest [40]

Formulation of the C_d and influenced parameters are presented in Equation 1 [41].

$$C_d = f\left(H, W, w, L_w, L_c, P, g, V, \sigma, \mu, \rho\right) \tag{1}$$

In which, L_w : total length of the crest of weir, L_c: length of one cycle, g: gravitational acceleration, σ: surface tension and ρ: density of flow and V is the mean velocity of flow. Using dimensional analysis such as Π theorem, the most important parameters that influence the C_d are derived as Equation 2. It is notable that due to installation W_L in particular of flow, therefore, the flow condition always is subcritical, moreover, in irrigation channel flow is turbulent and investigators try to remove the effect of surface tension. Therefore, Froude, Reynolds and Weber numbers can be negligible [42].

$$C_d = f\left(\frac{H}{P}, \frac{w}{W} = n, \frac{L_c}{W}, \frac{L_c}{w}\right) \tag{2}$$

The ratio of w/W and L_c/w introduces the Compression and elongation ratio. Preparation of artificial intelligent techniques are based on the dataset. Therefore, For this purpose, 223 data were extracted from various sources such as Ghodsian [42], Kumar, Ahmad and Mansoor [43]. The statistical properties of the extracted dataset is given in Table 1.

Table 1. The range of collected dataset related to triangular labyrinth weirs

Parameters range	Min	Max	Avg.	STDEV
Weir length	0.245	1.200	0.475	0.282
Channel width	0.245	0.300	0.271	0.019
Cycle width	0.123	0.280	0.213	0.075
Cycle length	0.123	1.082	0.373	0.263
Weir height	0.092	0.170	0.110	0.024
Total head	0.007	0.145	0.046	0.024
Discharge coefficient	0.148	0.906	0.595	0.172

2- 1- Multivariate Adaptive Regression Splines (MARS)

The MARS was come up with Friedman [44]. The MARS method categorized in non-parametric analysis of dataset. In MARS method, the features of dataset are divided into sub-domains and fitted splines to them to express a mathematical relation between independent and dependent variables. Mathematical form of derived formula from modeling using MRAS method is presented in Equation 3:

$$n = C_0 + \sum_{i=1}^{N} C_i \prod_{j=1}^{Kj} B_{ji}\left(y_{v(j,i)}\right) \tag{3}$$

In which, n is the desired parameter, C_0 is the constant value, C_i are the weight coefficients are multiplied in basis functions $B_{ji}\left(y_{v(j,i)}\right)$ is the truncated power basis function, $y_{v(j,i)}$ is the index of desired input parameters of the i^{th} term and j^{th} product and k_j is the limitation of interaction order. The mathematical form of fitted splines are presented in equation:

$$\begin{aligned} B_{ji}(y) &= \left(y - t_{ji}\right)_+^q = \begin{cases} \left(y - t_{ji}\right)^q, & y < t_{ji} \\ 0, & otherwise \end{cases} \\ B_{ji+1}(y) &= \left(t_{ji} - y\right)_+^q = \begin{cases} \left(y - t_{ji}\right)^q, & y < t_{ji} \\ 0, & otherwise \end{cases} \end{aligned} \tag{4}$$

Where t_{ji} is the loop of spline, developing the MARS model consist of two stages. Frist is dividing the feature space of the dataset into many computational sub-domains and fitting spline to them. In this stage that named the growth stage, many splines are developed and fitted. In the next step, to increase the efficiency and prevent of local performance of the model, the number of splines is removed. This stage named purned stage. Removing the splines is based on the ing the residual sum of squares (RSS) error for dataset which are assigned to the training stage. The RSS is calculated via the following equation:

$$RSS = \sum_{i=1}^{N} \left(n_i - f_i\right)^2 \tag{5}$$

In which, n_i is the observed data and f_i is the predicted data. The accuracy of basis function is measured by the generalized cross-validation (GCV) index that is calculated by the equation:

$$GCV = \frac{RSS}{N\left[1 - \frac{C(B)}{N}\right]^2} \tag{6}$$

In GCV index, the n is the number of dataset and C(B) is the penalty function that is calculated by the following equation:

$$C(B) = B + d\left(\frac{B-1}{2}\right) \tag{7}$$

where B is the number of the basis functions and d the penalty for each basis function term included to the model [44-47].

2- 2- Group Method of Data Handling (GMDH)

GMDH is a self-organized AI method that was offered by Ivakhnenko [48]. The idea of developing GMDH was derived from Volterra's series. According to this idea, the relation between the input and output of each complex system can be approximated by an infinite series of polynomials. The algebraic form of the Volterra series is presented in Equation 8.

$$y = w_0 + \sum_{i=1}^{n} w_i x_i + \sum_{i=1}^{n}\sum_{j=1}^{n} w_{ij} x_i x_j + \sum_{i=1}^{n}\sum_{j=1}^{n}\sum_{k=1}^{n} w_{ij} x_i x_j x_k + \cdots \tag{8}$$

Where, w_0, w_i, w_{ij},… are weights and x_i, x_j, x_k … are inputs. In the development of the first layer of GMDH network, pairs of inputs are introduced to neurons, individually. The number of neurons in the first layer is calculated as Equation 9.

$$\frac{n(n-1)}{2} \tag{9}$$

Where, n is input features. Ivakhnenko [48] stated that for modeling each complex system using GMDH network, a quadratic polynomial (Equation 9) of Volterra's series as the governing equation (transfer function) on the neurons is enough.

$$y = \varphi(x_i, x_j) = w_0 + w_1 x_i + w_2 x_j + w_3 x_i x_j + w_4 x_i^2 + w_5 x_j^2 \tag{10}$$

Figure 2 shows a sketch of the structure of GMDH neural network. As shown in Figure 2, the first layer of GMDH model assuming four inputs includes six neurons. For developing the next layers, competent neurons are selected to create the next layer. The competent criteria is defined based on their errors that are declared via root means square error (RMSE).

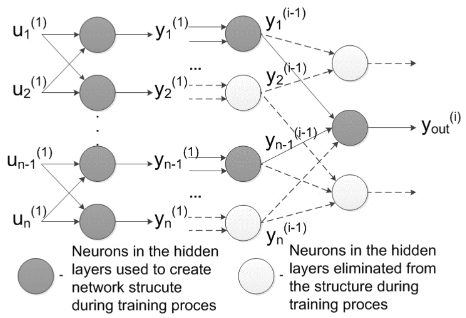

Figure 2. The scheme of the GMDH neural network

Justifying the weights can be assumed as optimization function. In other words, a function fitting problem should perform. To this end, the error (RMSE) of fitted function (governing equation on neurons) should be minimized.

2- 3- Genetic Programing

Genetic programming (GP) is a smart function fitting method the idea of which was based on the genetic algorithm. The main point about GP is the artificial evolution, which is a manifest characteristic of GP. This means that GP involved some artificial evolution such as genes, multigene, mutation and so on. GP has been widely used for function fitting in many fields of engineering and sciences, especially in water engineering for modeling scouring, water quality components, and discharge capacity of water convinces structure and so on. GP developed a new formula based on mathematical operators such as (+, −, /, and *) and functions such as (ex, x, sin, cos, tan, lg, sqrt, ln, power). GP conducts this operation by randomly generating a population of computer programs (represented by tree structures) and then mutating and crossing over the best performing trees to create a new population. Unlike conventional regression operation, where the researcher defines the structure of empirical formula, GP automatically creates the structure of developed formula called semi-empirical formula. The final developed formula that is resulted from summarization of multigene, consists of one or more genes that is called GP tree. To improve the performance of fitness (e.g. to reduce a model's sum of squared errors on a dataset), the genes are obtained increasingly. The final formula may be weighted linear or nonlinear. The optimal weights for the genes are automatically obtained using the ordinary least squares to regress the genes against output data. Figure 3 shows a pseudo formula obtained by GP technique. In this formula, y is the output and inputs are x1, x2 and x3 [49].

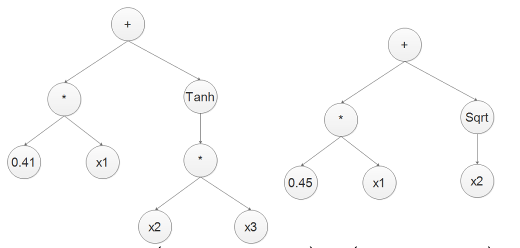

$$y = d_0 + d_1\left(0.41x_1 + \tanh\left(x_2 x_3\right)\right) + d_2\left(0.41x_3 + sqrt\left(x_2\right)\right)$$

Figure 3. A sketch of formula generation by GP technique

3- Results and Discussion

The purpose of this study was to model the discharge coefficient of the labyrinth weirs with a triangular plan using artificial intelligence techniques including GMDH, MARS and GP. These methods were selected since they are categorized as smart function fitting methods. This means that these methods using mathematical correlation process find most effective parameters on output and assign more weights to them during function fitting process. To develop GP, MARS and GMDH methods, the right side parameters of Equation 2 were considered as inputs and its left side (Cd) as output. To develop applied models, the dataset categorized into two classes as training and testing. Training was applied for calibration and testing dataset for validation. Eighty percent (80%=178) of collected dataset were assigned for calibration and the rest (20 percent=45) for validation. Random selection was considered for data allocating to each group. There is required to set some parameters of GP model for developing the mathematical formula of C_d of labyrinth weir with a triangular plan. The setting values of GP parameters are presented in Table 2.

Table 2. The values of Parameters required in the Genetic Programming

Parameter	Description of parameter	Setting of parameter
P1	Function set	times, minus, plus, square, tanh, exp,sin, cos
P2	Population size	200
P3	Mutation frequency %	0.94
P4	Crossover frequency %	50
P5	Number of replication	10
P6	Block mutation rate %	30
P7	Instruction mutation rate %	30
P8	Instruction data mutation rate %	40
P9	Homologous crossover %	95
P10	Program size	Initial 64, maximum 256

Genes obtained from developing stages of GP for mathematical expression of involved parameters on C_d, are presented in Figure 4. Observing Figure 4 shows that among the involved components used to model and predict C_d, H/P, Lw/Lc, and Lw/Wmc were used more compared to others. This shows that these parameters are more important. Mathematical derived formulas for genes are presented in Equations 11-14. The final mathematical formal obtained from GP technique is given in Equation 14. Results of GP technique in calibration and validation stages are presented in Figures 6 and 7.

Gene 1:

$$2.766 - 2.838 Sin\left(\tanh\left(Cos\left(P/H - 0.884\right)\right)\right) \tag{11}$$

Gene 2:

$$0.056\exp(\mathrm{Lw/Lc})(H/P - 1.232) + 0.056 Cos(\mathrm{Lc/Wc})\tanh(H/P)(P/H + 1.872) \tag{12}$$

Gene 3:

$$0.040 Cos\left(Lw/Lc\left(Lw/Wmc + 1.872\right)\right) - 0.040\left(Lw/Lc\right)\left(H/P + Lc/Wc\right) \tag{13}$$

General Form:

$$\begin{aligned} Cd &= 0.04\cos\left(Lw/Lc\left(Lw/Wmc + 1.872\right)\right) - 2.837\sin\left(\tanh\left(\cos\left(H/P - 0.885\right)\right)\right) - \\ &0.04 Lw/Lc\left(H/P + Lc/Wc\right) + 0.056\exp\left(Lw/Lc\right)\left(H/P - 1.232\right) + \\ &0.056\cos\left(Lc/Wc\right)\tanh\left(H/P\right)\left(H/P + 1.872\right) + 2.766 \end{aligned} \tag{14}$$

The model derived from GMDH model for modeling the C_d is given in Figure 5. The structure of the obtained network that forms GMDH model is shown in Figure 5. Results of the coefficient of governing neurons are given in Table 3. Attention to the structure of obtained GMDH model, especially neuron five in the first hidden layer that is a key neuron in obtained structure of model, shows that H/P, Lw/Lc, and Lw/Wmc are the most effective parameters on C_d. Previously, these results that obtained the most effective parameters on C_d were achieved using GP. Results of calibration and validation of the obtained model of GMDH technique are given in Figures 6 and 7. In these figures, the error indices including R-square (R^2) and root mean square error (RMSE) that their related equations have given in Equation 16 are shown, as well.

The results of the obtained model from MARS techniques are given in Table 4. Reviewing Table 4 indicated that the most effective parameters on C_d are H/P, Lw/Lc, and Lw/Wmc. The mathematical formula derived from MARS model is given in Equation 15. Results of MARS model during calibration and validation stages are shown in Figures 6 and 7. Development of MARS model for modeling C_d includes two stages. The first stage is called growing and the second is called pruning. The criterion in the pruning stage (GCV) was equal to (0.0022). At the first stage of MARS model development, thirty basic functions were developed, and in the pruning stage, fifteen functions were pruned. Obtained basic functions and their coefficients are given in Table 4.

$$C_d = 1.025 + \sum_{M=1}^{15} \beta_m BF_i(x) \tag{15}$$

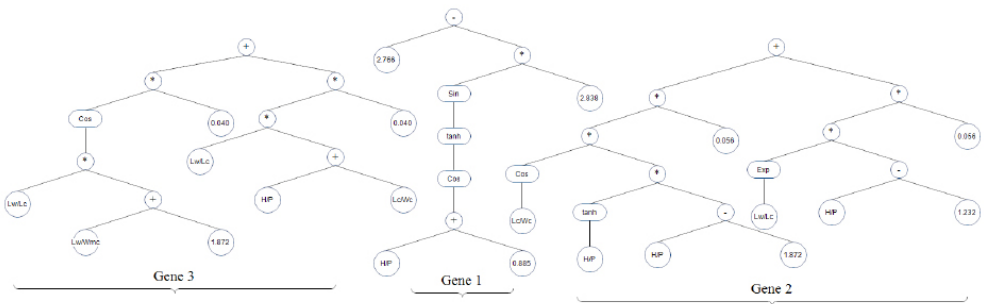

Figure 4. The structure of genomes derived from the genetic programming method

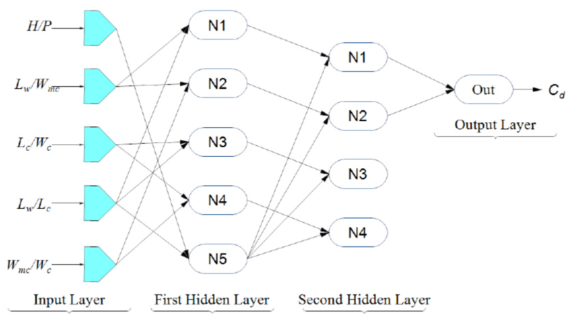

Figure 5. Obtained structure of GMDH model

Table 3. Coefficients of GMDH model for modeling the discharge coefficient

Layer	Neuron	b_0	b_1	b_2	b_3	b_4	b_5	RMSE
Layer-1	N_1 - 1	0.561	0.057	0.333	0.019	-0.124	-0.136	0.056
	N_1 - 2	0.561	0.057	0.333	0.019	-0.124	-0.136	0.056
	N_1 - 3	0.561	0.057	0.333	0.019	-0.124	-0.136	0.056
	N_1 - 4	0.561	0.057	0.333	0.019	-0.124	-0.136	0.056
	N_1 - 5	0.815	-1.626	0.452	1.342	-0.273	0.260	0.081
Layer-2	N_2 - 1	-0.471	2.694	0.022	0.435	3.004	-4.945	-0.004
	N_2 - 2	-0.471	2.694	0.022	0.435	3.004	-4.945	-0.04
	N_2 - 3	-0.471	2.694	0.022	0.435	3.004	-4.945	-0.04
	N_2 - 4	-0.471	2.694	0.022	0.435	3.004	-4.945	-0.04
Output	N_4 - 1	-0.011	0.522	0.522	-0.014	-0.014	-0.014	-0.011

Table 4. Mathematical model obtained from MARS method (basic functions and related coefficients)

Basic functions	Coefficients
BF1 = max(0, Lw/Lc-1) × max(0, Lw/Wmc-3)	0.359
BF2 = max(0, Lw/Lc-1) ×max(0, 3 - Lw/Wmc)	-0.113
BF3 = max(0, H/P-0.308)	-0.386
BF4 = max(0, Lw/Wmc-1.023)	-0.688
BF5 = max(0, 0.308 - H/P) × max(0, Lw/Wmc-2)	-46.494
BF6 = max(0, Lw/Lc-1) × max(0, H/P-0.308)	0.3166
BF7 = max(0, Lw/Lc-1) × max(0, 0.308 - H/P)	0.342
BF8 = max(0, 1.023 - Lw/Wmc) × max(0, 0.417 - H/P)	87.599
BF9 = BF3 max(0, Lw/Wmc-1.976)	0.194
BF10 = BF4 max(0, 2 - Lw/Lc`)	0.277
BF11 = max(0, 1.023 - Lw/Wmc) × max(0, 0.504-x1)	-76.852
BF12 = max(0, 3 - Lw/Wmc) × max(0, x3 -1.976)	-5.7694
BF13 = max(0, 3 - Lw/Wmc) max(0, 1.976 - Lc/Wc)	-0.121
BF14 = max(0, 0.308 - H/P) × max(0, Lw/Wmc-1.976)	46.530
BF15 = max(0, Lw/Wmc-1.414)	0.318

To prepare more details related to the outcomes of developed models throughout the dataset, developed discrepancy ratio (DDR) index, which was introduced by Noori, Ghiasi, Sheikhian and Adamowski [50] were calculated. This index is computed via Equation 16. This index declares the outcomes of applied models in terms of lower and over-estimation properties. Results of DDR for training and testing stages of developed models are shown in Figure 7. As shown in Figure 7, most amounts of data dispersion related to DDR index are related to GP model and the lowest data dispersion is related to the MARS, especially in testing stage. The accuracy of GMDH was less than MARS and more than GP. Reviewing Figure 7 shows that all three models have a bit over-estimation property.

$$DDR = \left(\frac{\text{Predicted Values}}{\text{Observed Values}}\right) - 1 \tag{16}$$

$$R^2 = \frac{\left(\sum_{i=1}^{n}\left(Cd_{obs} - \overline{Cd}_{obs}\right)\sum_{i=1}^{n}\left(Cdprd - \overline{Cd}_{prd}\right)\right)^2}{\sum_{i=1}^{n}\left(Cd_{obs} - \overline{Cd}_{obs}\right)^2 \sum_{i=1}^{n}\left(Cd_{est} - \overline{Cd}_{prd}\right)^2} \tag{17}$$

$$RMSE = \sqrt{\frac{1}{N}\sum_{i=1}^{N}(Cd_{obs} - Cd_{prd})}$$

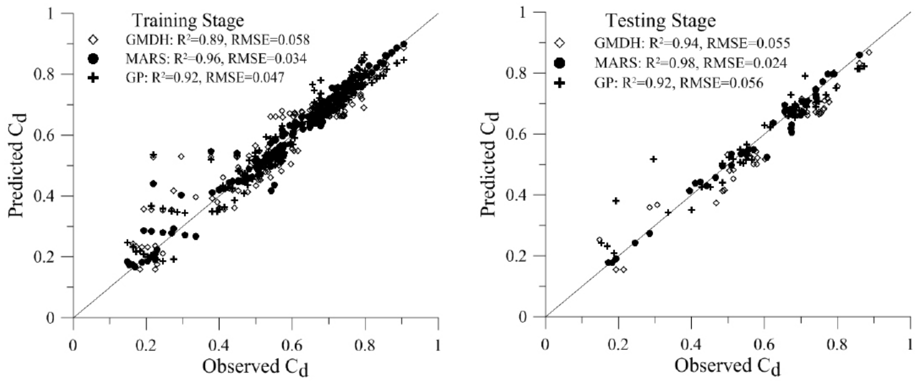

Figure 6. Results of applied models for predicting C_d versus observed data

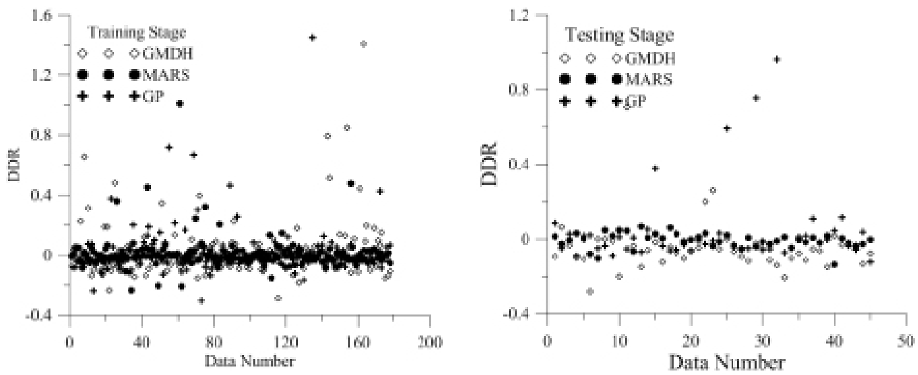

Figure 7. DDR index for results of applied models during training and testing stage

4- Conclusion

In this paper, the discharge coefficient of WL with a triangular plan was modeled and predicted using artificial intelligence techniques including GMDH, MARS and GP. These techniques were selected since they are categorized as smart function fitting methods. The main properties of smart function fitting methods are related to the definition of the most effective parameters on output and assigning more weights to them in modeling process. This characteristic causes an increase in the reliability of results of obtained models. In this study, observing the structure of obtained models from GMDH, MARS and GP, indicated that H/P, Lw/Lc, and Lw/Wmc were the most effective parameters on Cd of triangular WL. Assessment of the performance of developed models via calculation of error indices on results of applied models such as coefficient of determination and root-mean-square error indicated that all of them have suitable accuracy for practical purposes. However, MARS model is more accurate than others are. Evaluating the performance of applied models in terms of DDR index declared that data dispersivity of results of MARS model is less than others are and its results are more reliable.

Conflict of Interest

There is no conflict of interest.

Notations

W_L	Labyrinth Weir
AI	Artificial Intelligent
ANFIS	Adaptive Neuro-Fuzzy Inference System
ANN's	artificial neural networks
C_d	discharge coefficient
CFD	computational fluid dynamic
DDR	discrepancy ratio
GMDH	Group method of data handling
GP	genetic programing
MARS	multivariate adaptive regression splines
R^2	Coefficient of determination
RMSE	Root mean square error
SFF	smart function fitting method
SVM	Support Vector machine

References

[1] M. Ameri, A.A. Dehghani, A. Ahmadi, Elementary discharge coefficient of a triangular–rectangular sharp-crested side weir in subcritical flow, International Journal of River Basin Management, (2015) 1-8.

[2] J.P. Tullis, N. Amanian, D. Waldron, Design of Labyrinth Spillways, Journal of Hydraulic Engineering, 121(3) (1995) 247-255.

[3] S. Erpicum, F. Laugier, M. Pfister, M. Pirotton, G.M. Cicero, A.J. Schleiss, Labyrinth and Piano Key Weirs II, Taylor & Francis, 2013.

[4] B.P. Tullis, J.C. Young, M.A. Chandler, Head-Discharge Relationships for Submerged Labyrinth Weirs, Journal of Hydraulic Engineering, 133(3) (2007) 248-254.

[5] F.G. Tacail, B. Evans, A. Babb, Case study of a labyrinth weir spillway, Canadian Journal of Civil Engineering, 17(1) (1990) 1-7.

[6] M. Leite Ribeiro, M. Bieri, J.L. Boillat, A.J. Schleiss, G. Singhal, N. Sharma, Discharge Capacity of Piano Key Weirs, Journal of Hydraulic Engineering, 138(2) (2012) 199-203.

[7] R.M. Anderson, B.P. Tullis, Comparison of Piano Key and Rectangular Labyrinth Weir Hydraulics, Journal of Hydraulic Engineering, 138(4) (2012) 358-361.

[8] G. Taylor, The performance of labyrinth weirs, University of Nottingham, 1968.

[9] A.Y. Mohammed, Numerical analysis of flow over side weir, Journal of King Saud University - Engineering Sciences, 27(1) (2015) 37-42.

[10] M. Emin Emiroglu, M. Cihan Aydin, N. Kaya, Discharge Characteristics of a Trapezoidal Labyrinth Side Weir with One and Two Cycles in Subcritical Flow, Journal of Irrigation and Drainage Engineering, 140(5) (2014) 04014007.

[11] S. Bagheri, A.R. Kabiri-Samani, M. Heidarpour, Discharge coefficient of rectangular sharp-crested side weirs, Part I: Traditional weir equation, Flow Measurement and Instrumentation, 35 (2014) 109-115.

[12] H. Haddadi, M. Rahimpour, A discharge coefficient for a trapezoidal broad-crested side weir in subcritical flow, Flow Measurement and Instrumentation, 26(0) (2012) 63-67.

[13] O. Kisi, M. Emin Emiroglu, O. Bilhan, A. Guven, Prediction of lateral outflow over triangular labyrinth side weirs under subcritical conditions using soft computing approaches, Expert Systems with Applications, 39(3) (2012) 3454-3460.

[14] O. Castro-Orgaz, W. Hager, Subcritical Side-Weir Flow at High Lateral Discharge, Journal of Hydraulic Engineering, 138(9) (2012) 777-787.

[15] M.E. Emiroglu, H. Agaccioglu, N. Kaya, Discharging capacity of rectangular side weirs in straight open channels, Flow Measurement and Instrumentation, 22(4) (2011) 319-330.

[16] M. Ghodsian, Supercritical flow over a rectangular side weir, Canadian Journal of Civil Engineering, 30(3) (2003) 596-600.

[17] M. Jalili, S. Borghei, Discussion: Discharge Coefficient of Rectangular Side Weirs, Journal of Irrigation and Drainage Engineering, 122(2) (1996) 132-132.

[18] A. Corhay, S. Erpicum, F. Laugier, M.H.T. Khanh, M. Pfister, Labyrinth and Piano Key Weirs III: Proceedings of the 3rd International Workshop on Labyrinth and Piano Key Weirs (Pkw 2017), February 22-24, 2017, Qui Nhon, Vietnam, Taylor & Francis, 2017.

[19] S. Erpicum, F. Laugier, J.L. Boillat, M. Pirotton, B. Reverchon, A. Schleiss, Labyrinth and piano key weirs—PKW 2011, in: Proceedings of the International Conference on Labyrinth and Piano Key Weirs, Balkema Liege, 2011, pp. 9-11.

[20] S. Dehdar-behbahani, A. Parsaie, Numerical modeling of flow pattern in dam spillway's guide wall. Case study: Balaroud dam, Iran, Alexandria Engineering Journal, 55(1) (2016) 467-473.

[21] A. Parsaie, A.H. Haghiabi, Numerical Modeling of Flow Pattern in Spillway Approach Channel, Jordan Journal of Civil Engineering, 12(1) (2018) 1-9.

[22] Z. Kashkaki, H. Banejad, M. Heydari, Application of ANN in Estimating Discharge Coefficient of Circular Piano Key Spillways, Soft Computing in Civil Engineering, 2(3) (2018) 39-49.

[23] A. Parsaie, H.M. Azamathulla, A.H. Haghiabi, Prediction of discharge coefficient of cylindrical weir–gate using GMDH-PSO, ISH Journal of Hydraulic Engineering, 24(2) (2018) 116-123.

[24] E. Olyaie, H. Banejad, M. Heydari, Estimating Discharge Coefficient of PK-Weir Under Subcritical Conditions Based on High-Accuracy Machine Learning Approaches, Iranian Journal of Science and Technology, Transactions of Civil Engineering, (2018).

[25] A.H. Haghiabi, A. Parsaie, S. Ememgholizadeh, Prediction of discharge coefficient of triangular labyrinth weirs using Adaptive Neuro Fuzzy Inference System, Alexandria Engineering Journal, (2017).

[26] M.C. Aydin, CFD simulation of free-surface flow over triangular labyrinth side weir, Advances in Engineering Software, 45(1) (2012) 159-166.

[27] M.C. Aydin, M.E. Emiroglu, Determination of capacity of labyrinth side weir by CFD, Flow Measurement and Instrumentation, 29(0) (2013) 1-8.

[28] G.K. Robertson, Labyrinth weir hydraulics: Validation of CFD modelling, Stellenbosch: Stellenbosch University, 2014.

[29] B.M. Crookston, B. Tullis, Labyrinth weirs, Hydraulic Structures, (2010) 59.

[30] O. Bilhan, M. Emin Emiroglu, O. Kisi, Application of two different neural network techniques to lateral outflow over rectangular side weirs located on a straight channel, Advances in Engineering Software, 41(6) (2010) 831-837.

[31] I. Ebtehaj, H. Bonakdari, A.H. Zaji, H. Azimi, A. Sharifi, Gene expression programming to predict the discharge coefficient in rectangular side weirs, Applied Soft Computing, 35 (2015) 618-628.

[32] M.E. Emiroglu, O. Bilhan, O. Kisi, Neural networks for estimation of discharge capacity of triangular labyrinth side-weir located on a straight channel, Expert Systems with Applications, 38(1) (2011) 867-874.

[33] M. Najafzadeh, A. Etemad-Shahidi, S.Y. Lim, Scour prediction in long contractions using ANFIS and SVM, Ocean Engineering, 111 (2016) 128-135.

[34] A. Parsaie, H.M. Azamathulla, A.H. Haghiabi, Physical and numerical modeling of performance of detention dams, Journal of Hydrology, (2017).

[35] A. Parsaie, A.H. Haghiabi, M. Saneie, H. Torabi, Applications of soft computing techniques for prediction of energy dissipation on stepped spillways, Neural Computing and Applications, (2016) 1-17.

[36] A.H. Haghiabi, H.M. Azamathulla, A. Parsaie, Prediction of head loss on cascade weir using ANN and SVM, ISH Journal of Hydraulic Engineering, (2016) 1-9.

[37] A.H. Zaji, H. Bonakdari, Performance evaluation of two different neural network and particle swarm optimization methods for prediction of discharge capacity of modified triangular side weirs, Flow Measurement and Instrumentation, 40 (2014) 149-156.

[38] K. Roushangar, M.T. Alami, J. Shiri, M.M. Asl, Determining discharge coefficient of labyrinth and arced labyrinth weirs using support vector machine, Hydrology Research, 49(3) (2018) 924-938.

[39] H.M. Azamathulla, A.H. Haghiabi, A. Parsaie, Prediction of side weir discharge coefficient by support vector machine technique, Water Science and Technology: Water Supply, 16(4) (2016) 1002-1016.

[40] J. Mohammadzadeh-Habili, M. Heidarpour, S. Samiee, Study of Energy Dissipation and Downstream Flow Regime of Labyrinth Weirs, Iranian Journal of Science and Technology, Transactions of Civil Engineering, 42(2) (2018) 111-119.

[41] K. Gupta, S. Kumar, Z. Ahmad, FLOW CHARACTERISTICS OF SHARP-CRESTED W-PLANFORM WEIRS, World Applied Sciences Journal, 32(7) (2014) 1311-1317.

[42] M. Ghodsian, Stage–discharge relationship for a triangular labyrinth spillway, Proceedings of the ICE-Water Management, 162(3) (2009) 173-178.

[43] S. Kumar, Z. Ahmad, T. Mansoor, A new approach to improve the discharging capacity of sharp-crested triangular plan form weirs, Flow Measurement and Instrumentation, 22(3) (2011) 175-180.

[44] A. Haghiabi, Estimation of scour downstream of a ski-jump bucket using the multivariate adaptive regression splines, Scientia Iranica. Transaction A, Civil Engineering, 24(4) (2017) 1789-1801.

[45] A.H. Haghiabi, Prediction of longitudinal dispersion coefficient using multivariate adaptive regression splines, Journal of Earth System Science, 125(5) (2016) 985-995.

[46] A.H. Haghiabi, Modeling River Mixing Mechanism Using Data Driven Model, Water Resources Management, 31(3) (2017) 811-824.

[47] A. Parsaie, A.H. Haghiabi, M. Saneie, H. Torabi, Prediction of energy dissipation on the stepped spillway using the multivariate adaptive regression splines, ISH Journal of Hydraulic Engineering, 22(3) (2016) 281-292.

[48] A.G. Ivakhnenko, Polynomial theory of complex systems, IEEE transactions on Systems, Man, and Cybernetics, 1(4) (1971) 364-378.

[49] M.F. Brameier, W. Banzhaf, Linear Genetic Programming, Springer US, 2007.

[50] R. Noori, B. Ghiasi, H. Sheikhian, J.F. Adamowski, Estimation of the Dispersion Coefficient in Natural Rivers Using a Granular Computing Model, J. Hydraul. Eng., (2017) 04017001.

Please cite this article using:
A. H. Haghiabi, A. Parsaie, Z. Shamsi, Intelligent mathematical modeling of discharge coefficient of nonlinear weirs with triangular plan, *AUT J. Civil Eng.*, 3(2) (2019) 149-156.
DOI: 10.22060/ajce.2018.14833.5500